**Preprints.org**

Article

# Pilocarpine-Induced Status Epilepticus in the Rat Hippocampus is Associated with Reactive Glia and Concomitant Increased Expression of CD31, PDGFRβ and Collagen IV in Endothelial Cells and Pericytes of the Blood Brain Barrier

Grigorios Kyriatzis , Anne Bernard , Angélique Bôle , Michel Khrestchatisky [*] , Lotfi Ferhat [*]

*Article*

# Pilocarpine-Induced Status Epilepticus in the Rat Hippocampus is Associated with Reactive Glia and Concomitant Increased Expression of CD31, PDGFRβ and Collagen IV in Endothelial Cells and Pericytes of the Blood Brain Barrier

**Grigorios Kyriatzis** [1,#]**, Anne Bernard** [1]**, Angélique Bôle** [1]**, Michel Khrestchatisky** [1,*] **and Lotfi Ferhat** [1,*]

[1]  Aix-Marseille Univ, CNRS, INP, Institut de Neurophysiopathol, Marseille, France

[*]  Correspondence: Michel Khrestchatisky, Institute of Neurophysiopathology, INP, CNRS, Aix-Marseille University, Faculté de Médecine, 27 Bd Jean Moulin, 13005 Marseille, France. Tel: +33(0)4 91 69 87 29, e-mail: michel.khrestchatisky@univ-amu.fr; Lotfi Ferhat, Institute of Neurophysiopathology, INP, CNRS, Aix-Marseille University, Faculté de Médecine, 27 Bd Jean Moulin, 13005 Marseille, France. Tel: +33(0)4 91 69 87 29, e-mail: lotfi.ferhat@univ-amu.fr

[#]  Current address: Nea Karvali, 64006 Kavala, Greece. g.kyriatzis@gmail.com.

**Abstract:** Temporal lobe epilepsy (TLE) is associated with reorganization of neuronal networks, gliosis, neuroinflammation, loss of integrity of the blood brain barrier (BBB) in the hippocampus in humans and animal models. More than 30% of epilepsies remain intractable and characterization of the molecular mechanisms involved in BBB dysfunction is essential to the identification of new therapeutic strategies. In this work, we induced status epilepticus in rats by injection of the proconvulsant drug pilocarpine that leads to TLE. Using RT-qPCR, double immunohistochemistry and confocal imaging, we studied at different time points of epileptogenesis (latent phase, 3, 7, 14 days; chronic phase, 1 and 3 months) the regulation of reactive glia and vascular markers. In the hippocampus, increased expression of mRNA encoding the glial proteins GFAP and Iba1 confirmed neuroinflammatory status. We report for the first time the concomitant induction in endothelial cells, pericytes and basal membrane of the BBB of specific proteins CD31, PDGFRb and ColIV, that peaks at the same time points as inflammation. The altered expression of these proteins occurs early in TLE, during the latent phase, suggesting that they could be associated with early rupture and pathogenicity of the BBB that will contribute to the chronic phase of epilepsy.

**Keywords:** blood brain barrier; gliosis; temporal lobe epilepsy; inflammation; epileptogenesis; hippocampus; endothelial cells; pericytes; basal membrane

## 1. Introduction

Epilepsy is the third commonest neurological disorder, affecting more than 65 million people worldwide [1]. Despite progress in anti-epileptic treatments, up to 40% of epileptic patients remain resistant to all currently available therapies, and patients who respond to anti-epileptic treatments often complain of debilitating side effects [2]. Temporal lobe epilepsy (TLE), its commonest form that affects particularly the hippocampus, is characterized by the loss of principal neuronal cells and interneurons, structural reorganization such as sprouting, neo-spinogenesis and neurogenesis with cell dispersion, gliosis, neuroinflammation, and loss of the integrity of the blood-brain barrier (BBB) [3]. Each one of these characteristics has been observed in surgical or post-mortem samples obtained from patients with pharmaco-resistant TLE or from animal models of TLE [3–5]. The aforementioned histopathological alterations are thought to take place following an initial injury and contribute to

epileptogenesis [5,6]. The BBB is a cellular barrier made up of endothelial cells that line brain capillaries and that are encased in a basement membrane –or basal lamina–in interaction with pericytes, which are closely linked to brain parenchyma cells such as astrocytes, microglia, and neurons [7].

Cluster of differentiation 31 (CD31), also known as platelet endothelial cell adhesion molecule-1 (PECAM-1), platelet-derived growth factor receptor beta (PDGFRβ) and collagen IV (ColIV), are specific markers of principal cells that constitute the BBB. Indeed, CD31 is expressed mainly by brain microvascular endothelial cells, while PDGFRβ is specific of pericytes, contractile cells that surround endothelial cells and that control blood flow. Other major constitutive cells of the BBB are astrocytes, which interact with and surround endothelial cells and pericytes, in particular via specialized structures known as astrocytic end-feet. In the BBB, ColIV is the most abundant component of the basement membrane, and is produced predominantly by endothelial cells, pericytes and astrocytes [8].

The BBB protects the central nervous system (CNS) very efficiently. It is a selective filter between blood and brain parenchyma, it regulates the selective uptake of nutrients and proteins from the blood, the influx into the CNS of toxic xenobiotics and pathogens and the efflux of metabolic waste. BBB integrity is essential for CNS homeostasis, and many disorders of the CNS, including stroke, traumatic brain injuries, tumors, infectious and neurodegenerative diseases, entail BBB dysfunction [9]. Several studies suggest that BBB disruption may lead to epileptic seizures, and conversely, that seizures may further increase BBB demise [10–12]. Increased BBB permeability or leakage is one of the earliest characteristics of several brain diseases, including epilepsy [13,14]. BBB dysfunction may contribute to epileptogenesis via a cascade of events triggered by leakage of inflammatory mediators into the CNS, which causes neuroinflammation [15,16]. Alterations of different neuronal and glial populations of the brain parenchyma and their interactions have been extensively studied in epilepsy [17,18]. However, considerably less attention has been given to the regulation of molecular components involved in the integrity and stabilization of the BBB, notably in TLE.

In the present work, we induced status epilepticus (SE) leading to TLE in rats by injecting them with pilocarpine (PILO). We investigated the modulation of reactive glia and vascular markers at several time points of epileptogenesis (latent phase, 3, 7, 14 days; chronic phase, 1 and 3 months) using RT-qPCR, double immunohistochemistry, and confocal imaging. We report in the hippocampus of PILO-SE rats the increased expression of mRNA encoding the neuroinflammatory glial proteins GFAP and Iba1 and the concomitant induction in endothelial cells, pericytes and basal membrane of the BBB of specific proteins CD31, PDGFRβ and ColIV, respectively. These alterations could be associated with the rupture and pathogenicity of the BBB in TLE. Perivascular inflammation of reactive astrocytes and their end-feet in the PILO rat model was studied previously [19] and was not addressed in this study.

## 2. Methods

All experimental procedures involving rats were approved by National and European regulations (EU directive N° 2010/63) and were in agreement with the authorization for animal experimentation granted to the laboratory by the Prefecture des Bouches du Rhône (permit number: D 13 055 08) and to the project (N° 00757.02) by the French Ministry of Research and Local Ethics Committee.

Adult, male Wistar rats (200-290g) were first injected intraperitonally (i.p) with a low dose of the cholinergic antagonist scopolamine methyl nitrate (2 mg/kg; Sigma, Saint Louis, MO, USA) to minimize the peripheral effects of pilocarpine hydrochloride (PILO) (320 mg/kg; Sigma), a muscarinic cholinergic agonist diluted in 0.9% NaCl and administered i.p. 30 min after scopolamine. Control rats received an injection of 0.9% NaCl. At 1 h after the onset of SE, animals received diazepam (10 mg/kg, i.p.), and thereafter were carefully monitored to ensure a high survival rate. Only animals that developed sustained SE after PILO injection were included in this study. Among these animals, 90% of the PILO-treated animals developed spontaneous recurrent seizures (SRSs). Only seizures of grade 3 or greater on the Racine [20] scale were scored (i.e., forelimb clonus ± rearing ± falling). PILO-treated

animals were studied at several post-injection intervals: during the latent period, when animals displayed no behavioral seizures (3, 7 and 14 days), and during the chronic stage, when the animals developed SRSs (1 and 3 months). Each group of PILO-treated animals was compared to saline-treated rats used as controls. Histological and RT-qPCR observations were based on 18 PILO rats and 6 control saline-injected rats.

Following induction of SE, animals were subjected to a standard perfusion fixation protocol with NaCl, followed by 4% Antigenfix (paraformaldehyde-based; Diapath, Italy). Brains were then postfixed for 24 h in the same fixative solution and cryoprotected in 30% sucrose solution (Sigma) in phosphate buffer (PB) 0.12 M, and serial cryostat frozen sections of 40 μm thickness were cut and double-stained with anti-CD31 (PECAM-1; mouse, Abcam ab64543, 1:100, Cambridge, UK) and either PDGFRβ (rabbit, Abcam ab32570, 1:100) or Collagen IV (ColIV; goat, Southern Biotech 1340-01, 1:250, Birmingham, AL, USA). This antibody detects ColIVa1 to ColIVa6 and among these antigens, ColIVa1 and ColIVa3 are expressed in brain vascular tissue. Sections were permeabilized and saturated with PB 0.12 M containing 3% BSA-0,3% Triton X-100 for 1 h at RT. They were stained with the first primary antibody in PB 0.12 M, 3% BSA overnight (o/n) at 4oC, washed 3x PB 0.12 M, stained with the second primary antibody, washed 3x in PB 0.12 M. The ColIV and CD31 labeling were revealed with a donkey anti-goat AlexaFluor A488 and donkey anti-mouse AlexaFluor A594 (1:800) respectively for 2 h at RT in dark. The PDGFRβ immunolabeling was revealed with a goat anti-rabbit biotin (1:200) for 2 h at RT followed by streptavidin AlexaFluor A488. Tissue sections were washed 3x in PB 0.12 M, counterstained with DAPI for 30 min at RT in dark, mounted on glass slides using Fluoromount-G Mounting medium (Thermo Fisher Scientific, Dardilly, France) and stored at -20oC. Immunohistochemical controls for double-labeling experiments included incubation of some sections in a mixture of a primary antibody and normal IgG (mouse/goat/rabbit normal IgG). In all cases, these sections exhibited the same pattern of immunolabeling as sections processed for single labeling. Methods are described in detail in [19].

All cytochemical quantifications were performed blindly. Acquisitions were performed using a confocal laser-scanning LSM 700 Zeiss microscope and ZEN software (Zeiss, Jena, Germany). The mosaic function was used to visualize the whole hippocampus. All stained blood vessels of the dentate gyrus (DG) and the lacunosum-moleculare (LM), from 3 control (CTL) and 3 PILO-treated rats at 3 days post-SE (PILO 3D), were quantified for their mean fluorescence intensity in and around blood vessels using ImageJ software for the 3 markers as described in [19]. The mean fluorescence intensity was measured in blood vessels, by drawing and measuring around the inner and outer surface of various sized and shaped vessels and arterioles that were morphologically identified clearly. All vessels from 3 CTL and 3 PILO 3D rats were quantified. Background fluorescence was set in the stratum radiatum (SR), in areas devoid of brain vessels in the same sections and was subtracted. An average value of 3 such areas was obtained from every image. Data are presented as the average fluorescence intensity of PDGFRβ, CD31, or ColIV, relative to CTL (percentage). Images were processed using Adobe Photoshop software. Using ImageJ, the fluorescence intensity profiles (arbitrary units, A.U.) as a function of distance (pixels) (as described in [21–23]), were obtained for PDGFRβ and CD31 to determine whether the different markers stain distinct cell types of the BBB.

RNA extraction and RT-qPCR were performed on rat hippocampal tissue of CTL and PILO-treated rats on days 3, 7, 14 and on months 1 and 3 post-SE as described in [19]. RPL13, Ribosomal Protein L13, was used as internal mRNA reference. All reactions were performed using TaqMan Fast Universal PCR Mix (Applied Biosystems) and TaqMan Assays (Applied Biosystems) probes (Table 1). For the RT-qPCR experiments, we selected primers that detect the ColIVa1 and ColIVa3 mRNAs encoding the vascular isoforms of ColIV.

All experiments were performed at least 3 times with different rat series. One-way ANOVA analysis followed by Dunnett's *post hoc* test was used to compare the mean of each group with the mean of a CTL group. Unpaired Student's *t*-test was used to compare 2 groups. All data are expressed as the mean ± SEM. Statistical significance was set at $p < 0.05$. Histograms and statistical analyses were performed with PRISM GraphPad statistical software.

**Table 1.** Rat TaqMan probes used for qPCR analysis.

| Gene name | Gene description | Probe ID |
|---|---|---|
| *Gfap* | Glial fibrillary acid protein | Rn01253033 |
| *Iba1* | Ionized calcium binding adaptor molecule1 | Rn00574125 |
| *CD31 or PECAM-1* | EndoCAM or Platelet endothelial cell adhesion molecule-1 | Rn01467262 |
| *PDGFRβ* | Platelet-derived growth factor beta | Rn01502596 |
| *ColIV a1* | Collagen, type IV, a1 | Rn01482927 |
| *ColIV a3* | Collagen, type IV, a3 | Rn01400991 |
| *RPL13* | Ribosomal Protein L13 | Rn00821258 |

## 3. Results

All rats that were injected with PILO and that survived developed SE (mortality rate was around 25%). From 10 min to 1 h following PILO injection, rats exhibited limbic motor seizures every few minutes. At 3 weeks, SRSs started to appear that could last up to 60 seconds, and developed into generalized seizures within the following days, that persisted for the lifetime of the animals, in agreement with previous studies [19,24–27]. We could not address the specific effect of PILO without SE considering that all rats treated with PILO had SE. Considering that disruption of the BBB and neuroinflammation have been observed in several models of TLE and other pathologies, we can affirm that it is not the PILO treatment *per se* that leads to alteration of the BBB, but rather the SE induced by PILO.

We studied in the hippocampus, at different time points after PILO-induced SE (3, 7, 14 days, 1 and 3 months) (Figure 1 and Table 1), the expression of mRNAs encoding different neuroinflammatory and BBB markers. In particular, we assessed the inflammatory and reactive glial markers GFAP and Iba1, and the vascular markers CD31, specific of endothelial cells, PDGFRβ, specific of pericytes, and ColIVa1 and ColIVa3, specific of the BBB basal lamina [28]. GFAP and Iba1 mRNA were increased at the latent phase (3, 7 and 14 days) after PILO SE, and decreased at the chronic phase (1 and 3 months) after PILO SE. The mean GFAP and Iba1 mRNA levels were significantly increased in PILO rats when compared with CTL rats ($p<0.01$; Dunnett's test). Specifically, in PILO 3D, increases were ~11- and ~3-fold for GFAP and Iba1, respectively. In PILO 7D, GFAP and Iba1 increased ~9.7- and ~6-fold, respectively, whereas in PILO 14D, GFAP and Iba1 increased ~8- and ~5.7-fold, respectively. In PILO 1M, GFAP increased ~8-fold, whereas no difference was found for GFAP in PILO 3M and for Iba1 in PILO 1M and 3M (see histograms A and B, Figure 1). It is known that neuroinflammation may lead to alterations of the BBB [4,29]. Consistently, our data show that the upregulation of GFAP and Iba1 mRNA is associated with the significant increase of mRNAs encoding CD31 (PILO 3D and 7D, ~1.5-fold), PDGFRβ (PILO 7D, ~1.3-fold), and ColIVa1 (PILO 3D: ~2.2-fold; 7D: 1.8-fold). This upregulation follows the same temporal course as that of the reactive glia markers although at different levels, suggesting that CD31, PDGFRβ, and ColIVa3 are involved in inflammatory processes at the BBB.

RT-qPCR on rat hippocampal tissue
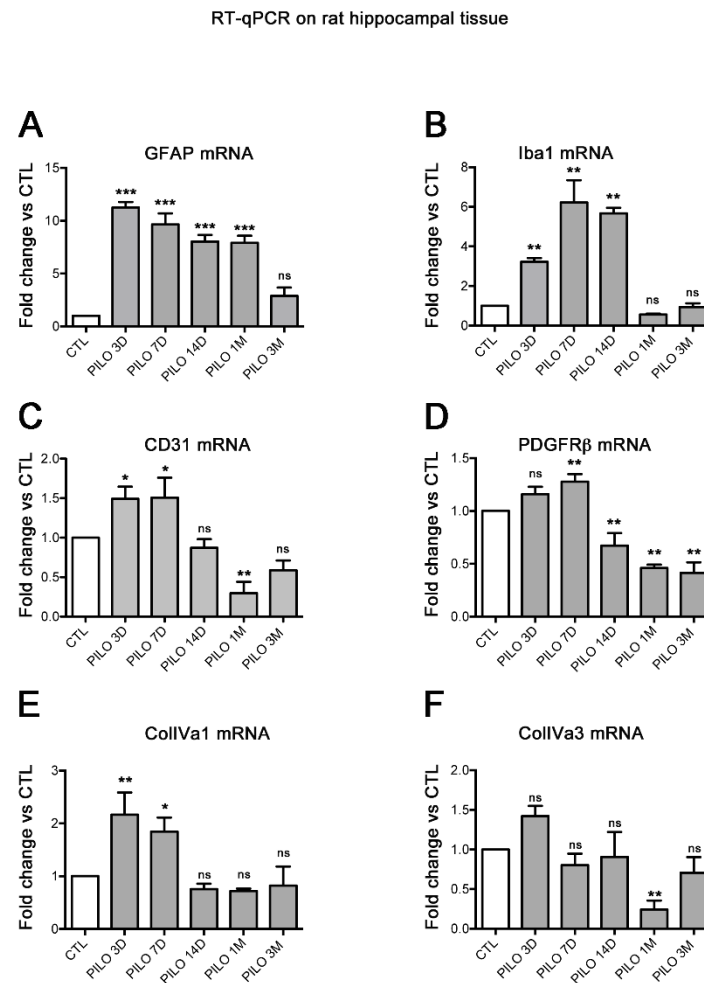


**Figure 1.** Histograms showing RT-qPCR quantification of the mean levels of mRNAs encoding the reactive glia markers GFAP (**A**), Iba1 (**B**) and the vascular markers CD31 (**C**), PDGFRβ (**D**), ColIVa1 (**E**) and ColIV a3 (**F**) at different time points after PILO-SE. In PILO-SE rats, GFAP and Iba1 mRNA were increased at early time points (latent phase, 3, 7 and 14 days) and decreased at the chronic phase (1 and 3 months) after PILO-SE. The expression of CD31, PDGFRβ and ColIVa1 mRNA follows the same trend as the glial markers. ColIVa3 mRNA levels were unchanged at early time points after PILO-SE but were decreased in the chronic phase at 1 month. Values are given as the mean ± SEM normalized to CTL. Asterisks indicate statistically significant differences: * $p<0.05$, ** $p<0.01$, ** $p<0.001$ (one-way Anova followed by Dunnett's *post hoc* test); ns: not significant; n=3 rats for each time point.

We next analyzed at the protein level, the regulation of the BBB markers assessed above by RT-qPCR, using immunohistochemistry with PDGFRβ, CD31, and Collagen IV (ColIV) antibodies. To this end, we first performed dual PDGFRβ and CD31 immunohistolabeling in CTL and PILO 3D rats (Figure 2A-C, F-H). At low magnification, in all areas and layers of the hippocampus of CTL rats, weak to moderate PDGFRβ staining was observed in neural cells (Figure 2A,C). Note that numerous cells were also stained in the subgranular zone of the DG, both in CTL and PILO 3D rats. In addition, moderate PDGFRβ expression was also observed in blood vessels of all sizes and shapes (see insets in Figure 2A,C). PDGFRβ and CD31 staining were increased in all hippocampal areas and layers of PILO 3D rats, as shown by mosaic tile scans (Figure 2F,H). Indeed, increased PDGFRβ was observed in the oriens (O), pyramidal layer (P), radiatum (R), lacunosum-moleculare (LM), molecular layer (M), and in the dentate gyrus (DG). In CTL rats, immunohistochemical analysis of rat brain sections showed CD31 immunoreactivity in blood vessels of all sizes and shapes (Figure 2B,C), which

increased in PILO 3D LM blood vessels, as well as in the CC (corpus callosum), O, P, and R, in PILO 3D animals (Figure 2G,H).

In the same line, we performed ColIV immunolabeling in CTL and PILO 3D rats (Figure 2D-E, I-J). In CTL rats, ColIV staining was observed only in the M of the DG lower blade (Figure 2D,E), whereas PILO 3D rats displayed strong labeling of the vasculature in the O, P, R, LM and M of the DG (Figure 2I,J). We refined our study by conducting semi-quantitative analysis in CTL and PILO 3D rats, to determine the extent of changes in the fluorescence intensity of the different vascular markers (Figure 2K). In PILO 3D animals, the expression of all vascular markers increased significantly in the blood vessels of the DG and the LM compared to CTL animals. Specifically, PDGFR$\beta$, CD31 and ColIV increased 1.4-, ~2 and ~1.9-fold respectively (Figure 2K, $p<0.001$, Student's $t$-test).
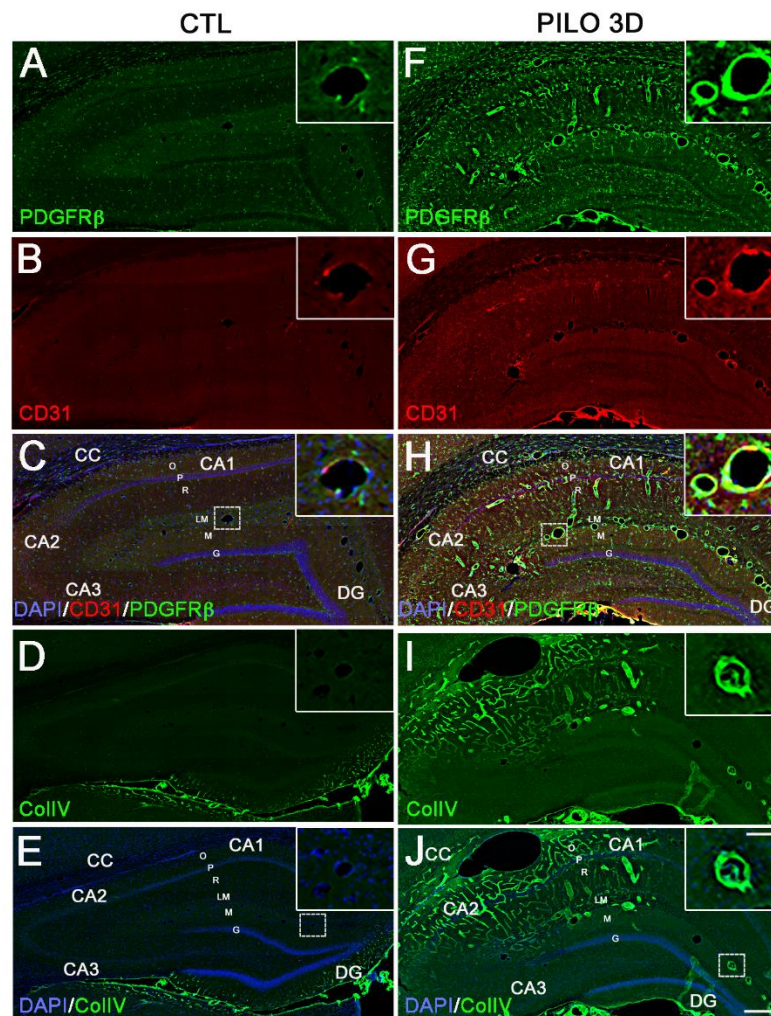
**Figure 2**. PDGFRβ, CD31 and ColIV protein expression increased in rat hippocampus following PILO-SE. A-J: PDGFRβ (green) and CD31 (red) double immunolabeling was performed in CTL (**A**-**C**) and PILO-treated rats at day 3 post-SE (PILO 3D, **F-H**). Similarly, ColIV (green) immunolabeling was performed in CTL (**D,E**) and PILO 3D rats (**I-J**). Cell nuclei were counterstained with DAPI (blue, **C,E,H,J**). CC, corpus callosum; O, stratum oriens; P, pyramidal neurons of CA1, CA2, and CA3; R, stratum radiatum; LM, stratum lacunosum-moleculare; M, molecular layer; DG, dentate gyrus; G, granule cell layer of the DG; H, hilus of the DG. PDGFRβ, CD31 and ColIV are markers of pericytes, endothelial cells and basal membrane respectively. PDGFRβ staining was detected in the hippocampus of CTL rats (**A,C**) and increased in PILO 3D rats, particularly in and around blood vessels (F,H). CD31 staining was concentrated in blood vessels of the LM (**B,C**) in CTL animals and increased significantly in LM blood vessels as well as throughout O, P and R in PILO 3D rats (**G,H**). Weak ColIV staining was observed in the rat CTL hippocampus, in particular in blood vessels of the LM (**D,E**), whereas prominent labeling of the vasculature was noted in PILO 3D rats, in O, P, R, LM, M and DG (**I,J**). Scale bars: 250 μm. K: Quantification of increased PDGFRβ, CD31 and ColIV proteins in rat blood vessels following PILO-SE. Histograms showing average percentage of the fluorescence intensity of these 3 markers in DG and LM vessels in CTL and PILO 3D rats (**K**). Blood vessels of PILO 3D rats expressed significant PDGFRβ, CD31 and ColIV levels compared to CTL vessels. PDGFRβ, CD31 and ColIV levels were increased compared to CTL. Values are given as the mean ± SEM as a percentage of CTL. Asterisks indicate statistically significant differences: *** $p<0.001$ (Student's *t*-test).

We used high magnification to analyze in detail the double immunolabeling of CD31 (red) and ColIV (green) in CTL animals compared with PILO 3D rats (Figure 3). The LM blood vessels displayed lower immunolabeling of CD31 (red) and ColIV (green) in CTL animals (A-F) when compared with PILO 3D rats (G-L). Increased CD31 and ColIV immunolabeling appeared within endothelial cells (red; arrows), and the basal lamina (green), respectively, as illustrated by higher magnification of the boxed-in area in L (M-R). Indeed, ColIV immunostaining was closely associated with CD31 staining (Figure 3M-R), with basal lamina surrounding endothelial cells as reported elsewhere [30,31]. In conclusion, in rat PILO 3D hippocampus, both CD31 and ColIV proteins were increased in rat blood vessel endothelial cells and basal membrane, respectively. Last, high magnification of CD31 (red) and PDGFRβ (green) double immunolabeling (Figure 4) show that the LM blood vessels displayed lower CD31 and PDGFRβ expression in CTL animals (A-F) when compared with PILO 3D rats (G-L).
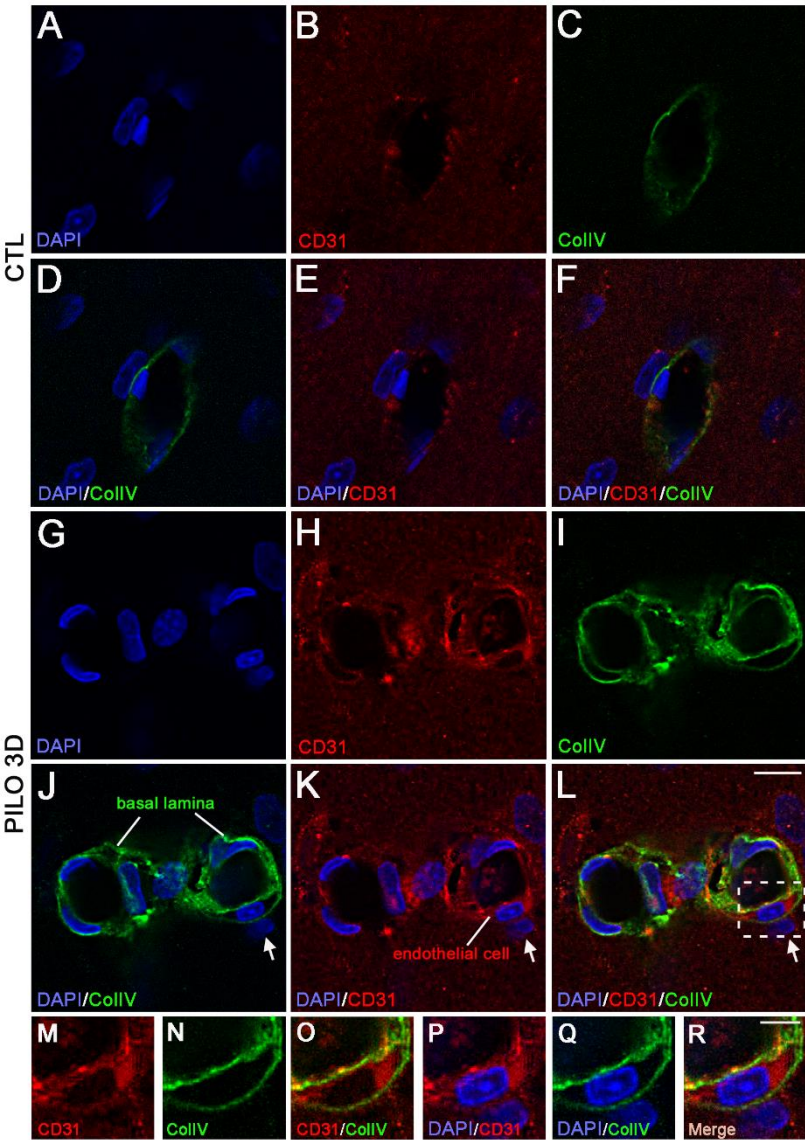
**Figure 3.** Double immunostaining followed by high magnification of LM blood vessels showed higher immunolabeling of CD31 (red) and ColIV (green) in PILO 3D rats (**G-L**) compared to CTL animals (**A-F**). Increased CD31 and ColIV occurred essentially within endothelial cells (red, arrows), and the basal lamina (green) respectively, as illustrated by higher magnification of the boxed-in area in L (**M-R**). Cell nuclei were counterstained with DAPI (blue). Scale bars: 10 μm in (**A-L**) and 5 μm in (**M-R**).
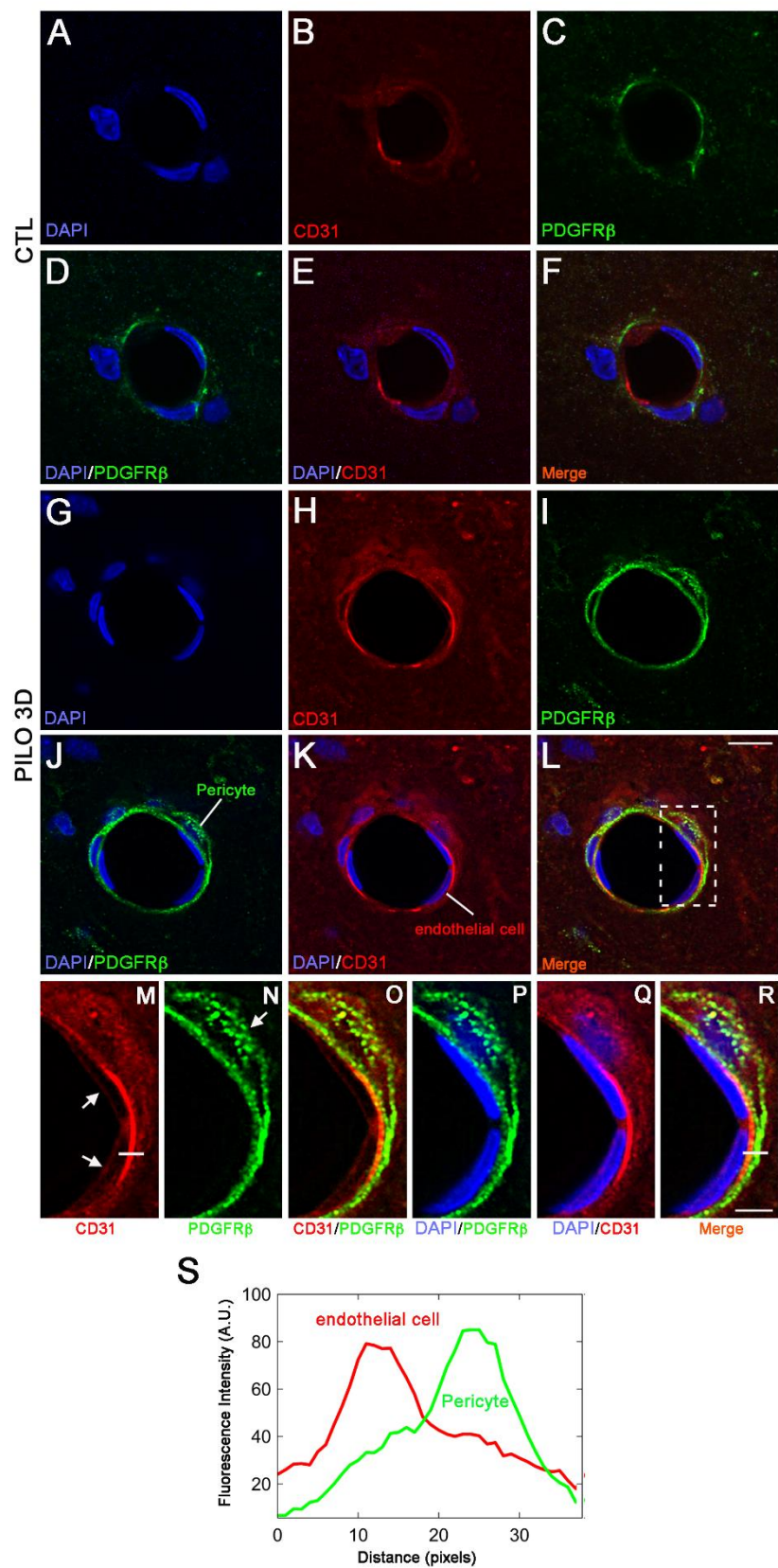
**Figure 4.** Double immunostaining followed by high magnification of LM blood vessels showed higher immunolabeling of CD31 (red) and PDGFRβ (green) in PILO 3D rats (**G-L**) compared to CTL animals (**A-F**). Increased CD31 and PDGFRβ occurred essentially within endothelial cells (red), and pericytes (green) respectively, as illustrated by higher magnification of the boxed-in area in L (**M-R**). Cell nuclei were counterstained with DAPI (blue). Scale bars: 10 μm in (**A-L**) and 5 μm in (**M-R**). White lines in

M and R insets are representative scans across the cell-cell borders along which fluorescence intensity profile (arbitrary units, A.U.) in relation to distance (pixels) were obtained to determine whether CD31 and PDGFRβ markers indeed stained endothelial (red line) and pericytes (green line) respectively.

It has been shown that PDGFRβ pericytes surround endothelial cells and are found between the abluminal surface of the endothelial tube and the basement membrane. Also, CD31 endothelial cells stain at the inner lining of blood vessels, while they are located between the basement membrane and the abluminal surface of the endothelial tube [30,31]. When analyzed at high magnification, the boxed-in region in L showed endothelial cells (red, arrows) encircled by a pericyte (green, arrow) (Figure 4M-R). To confirm that indeed CD31 and PDGFRβ were expressed in distinct cell types, kymographs were constructed and analyzed with ImageJ software from single-pixel width white lines taken from each channel of the confocal images (Figure 4K). Then, profiles of the signal intensities of CD31 (red line, K) and PDGFRβ (green line, K) were measured along the single-pixel width white lines drawn in (M) and (N), showing that immunolabeling of the two proteins is clearly distinct (Figure 4S). Thus, our results indicate that in PILO 3D, both CD31 and PDGFRβ increased specifically in endothelial cells and pericytes, respectively.

## 4. Discussion

In our present work, we investigated in the hippocampus the regulation of the neuroinflammatory GFAP and Iba1 markers and vascular proteins of the BBB such as CD31, PDGFRβ and ColIV, during the different phases of epilepsy. We used a well-characterized experimental model of TLE induced by PILO in adult rats and implemented RT-qPCR, immunohistochemical, and confocal microscopy techniques for analysis. This PILO model was selected because it involves a dynamic reorganization of neuronal networks, gliosis, neuroinflammation, loss of integrity of the BBB and neurovascular rearrangements in the hippocampus. This reorganization begins after the initial period of SE following PILO injection, during the silent period/latent phase when animals display a normal behavior, and reaches a plateau at the chronic phase when the animals develop SRSs [3–5,32].

In the PILO treated rats, we used RT-qPCR to study the kinetics of mRNAs coding for 2 reactive glial markers, GFAP and Iba1. We observed that mRNA levels of both markers were significantly increased in the hippocampus, at latent phase and decreased at chronic phase. These results are in agreement with previous studies [19,33–35] and confirmed neuroinflammation in our PILO rats.

The upregulation of glial markers in the hippocampus was accompanied by increased CD31, PDGFRβ and ColIVa1 mRNA, and concomitant protein expression at latent phase, when inflammation peaks (increased GFAP and Iba1) and decreased at the chronic phase (1 and/or 3 months), when glia reactivity subsides. CD31, PDGFRβ and ColIVa1 proteins were also increased in cells of the BBB.  These findings demonstrate that in this rat model of TLE, all 3 markers exhibit a significant increase, which may be indicative of structural alteration or remodeling of the BBB or neuroprotection mechanisms. Our results question whether the 3 BBB markers whose expression is upregulated in our epilepsy model are beneficial or detrimental for vascular integrity.

CD31 is mainly expressed by brain microvascular endothelial cells. This protein is a cell-cell adhesion and signaling molecule involved in angiogenesis and transmigration [36]. In agreement with our results, CD31 was induced in cerebral blood vessels between 24 and 72 h after Kainate administration in a mouse model of TLE [37]. It has been reported that peripheral and central inflammation promote breakdown of the BBB due to the upregulation of inflammatory mediators [38]. Hence, the increased expression of the vascular proteins we observed may be involved in the breakdown of the BBB in PILO rats. However, BBB components may also be key players in the pathogenicity of TLE, independently of inflammation. For instance, the expression of CD31 by CNS endothelial cells is not required for inflammation initiation and clinical signs in an animal model of multiple sclerosis [39]. CD31 maintains vascular integrity during inflammation by engaging into pro-survival pathways and by inhibiting cytokine production and pro-inflammatory signaling [40,41].

Accordingly, CD31 induction in our TLE model may be associated with anti-inflammatory and neuroprotection processes.

PDGFRβ is a marker of pericytes that are spatially isolated contractile cells on capillaries that control cerebral blood flow and BBB function in physiopathological conditions. A potential mechanism of pericyte action is the regulation of signaling through PDGFRβ that regulates pericyte survival, proliferation and migration signals. In TLE, we observed increased PDGFRβ expression in hippocampal blood vessels as expected, but also in parenchymal cells, suggestive of rearrangement in PDGFRβ distribution. The morphology and the distribution of these cells in all areas of the hippocampus including in the CC are reminiscent of glial cells. This observation is in agreement with Shen and colleagues [42] who detected PDGFR-β expression in cultured astrocytes isolated from neonatal mouse brain. Note that numerous cells were also stained in the subgranular zone of the DG both in CTL and PILO 3D rats, suggesting that PDGFRβ may be expressed in newly formed granule cells of the DG. Consistent with this observation, PDGFRβ is reported to be expressed in some neurons [42,43–45]. Outside the CNS, PDGFRβ expression has been proposed as a rescue response to cardiac vascular pathological insult [46]. In agreement with our results, Klement and colleagues [47] showed PDGFRβ mRNA increase in a mouse model of TLE induced by Kainate. In addition, within the regional scar that is a hallmark of epilepsy, a fibrotic-like PDGFRβ mesh was shown to develop around the capillaries, peaking at early stages post-SE, and regressing, but not resolving during the SRSs. Sakai and colleagues showed that the increased expression of PDGFRβ in the hippocampus after traumatic brain injury may lead to hypersensitivity to pilocarpine in a relevant mouse model [48]. PDGFRβ was proposed as a possible pharmacological target in epilepsy and the PDGFRβ agonist PDGF-BB reduced mural cell loss, vascular pathology and epileptiform activity [47–49]. In brain specimens of patients with TLE and hippocampal sclerosis (TLE-HS), increased perivascular PDGFRβ positive pericytes and enlarged and tortuous vessels were observed compared to TLE-non HS. Similarly, brain specimens derived from epileptic subjects affected by intractable seizures associated with focal cortical dysplasia (FCD) displayed high perivascular PDGFRβ immunoreactivity, typical of pericytes, and revealed ramified PDGFRβ positive cells proximal to microvessels [50]. The decreased expression of PDGFRb from PILO 14D to PILO 3M may be due to the loss of mural pericytes known to occur in epilepsy [49].

Our results are also reminiscent of the expression of PDGFRβ in brain specimens of patients affected by drug resistant epilepsy where the increased expression and rearrangement of PDGFRβ labeling after SE suggest the involvement of pericytes in cerebrovascular modifications associated with epilepsy [51,52]. In all, PDGFRβ labeling in animal experimental and human epileptic tissue is increased and appears to undergo distribution rearrangements in diseased tissue, indicating microvascular-pericyte-glia changes, scar formation, and inflammation in the epileptic pathology. However, it is difficult at this point to state whether PDGFRβ induction and rearrangement is beneficial or detrimental during SE or SRSs for the BBB and nervous tissue parenchyma.

ColIV is the most abundant component of the basement membrane (BM) of endothelial and epithelial cells. In the brain, ColIV is produced predominantly by brain endothelial cells and pericytes and these cells are separated by a BM. Six ColIV alpha chains (ColIV4a1 to ColIV4a6) have been identified. We studied specifically ColIVa1 and ColIVa3 that are involved in brain vascular integrity [8]. Increased ColIV has been shown in brain blood vessels in mouse, rat and sheep animal models and human stroke tissue [53]. Collagen IV induction was shown inside fibrotic scars [54], and following spinal cord injury in rats, where it may participate in glial scar formation [55]. An association has also been shown between seizures and deposition of collagen in porcine brain with taenia-solium neurocysticercosis [54]. ColIV was increased in other models of pathology, but around rather than in the microvasculature in rat chronic hypertension [56] and ColIV expression has been shown in brains of TLE patients, albeit outside the vasculature and in meninges [57]. We thus find some discrepancies on vascular vs perivascular ColIV distribution in our aforementioned results, considering that at the time points we studied, ColIV labeling was predominantly vascular in rat TLE. Interestingly, in epilepsy, collagen has been shown to have migrational properties, both *in vitro* and *in vivo*, on cells of the DG layer [58]. Since collagen is involved in scar formation typically associated

with experimentally induced epilepsy [59], one can hypothesize that the increased ColIV that we observe in epileptic hippocampi is involved in TLE-associated scar formation, but also in the migration of cells, in particular dentate granule neurons that play a critical role in SRSs.

In conclusion, our data confirm that in brain diseases such as TLE with obvious reactive glial inflammation, glial scar formation, neuronal network reorganization and BBB dysfunction, several BBB proteins such as CD31, PDGFR and ColIV are increased. It is difficult at this point to infer whether this increase and distributional rearrangements are detrimental or beneficial for BBB and brain parenchyma homeostasis. However, future research exploring more components that control BBB pathophysiological properties will help towards characterization of the cellular and molecular mechanisms that control vascular integrity, the basis of BBB dysfunction during epilepsy, and the development of new therapeutic strategies.

## References

1. Baulac, M.; de Boer, H.; Elger, C.; Glynn, M.; Kälviäinen, R.; Little, A.; Mifsud, J.; Perucca, E.; Pitkänen, A.; Ryvlin, P. Epilepsy Priorities in Europe: A Report of the ILAE-IBE Epilepsy Advocacy Europe Task Force. *Epilepsia* **2015**, *56*, 1687–1695, doi:10.1111/epi.13201.

2. Ayalew, M.B.; Muche, E.A. Patient Reported Adverse Events among Epileptic Patients Taking Antiepileptic Drugs. *SAGE Open Med.* **2018**, *6*, 2050312118772471, doi:10.1177/2050312118772471.

3. Ferhat, L. Potential Role of Drebrin a, an f-Actin Binding Protein, in Reactive Synaptic Plasticity after Pilocarpine-Induced Seizures: Functional Implications in Epilepsy. *Int. J. Cell Biol.* **2012**, *2012*, 474351, doi:10.1155/2012/474351.

4. Reddy, D.S.; Kuruba, R. Experimental Models of Status Epilepticus and Neuronal Injury for Evaluation of Therapeutic Interventions. *Int. J. Mol. Sci.* **2013**, *14*, 18284–18318, doi:10.3390/ijms140918284.

5. Curia, G.; Lucchi, C.; Vinet, J.; Gualtieri, F.; Marinelli, C.; Torsello, A.; Costantino, L.; Biagini, G. Pathophysiogenesis of Mesial Temporal Lobe Epilepsy: Is Prevention of Damage Antiepileptogenic? *Curr. Med. Chem.* **2014**, *21*, 663–688, doi:10.2174/0929867320666131119152201.

6. Weissberg, I.; Reichert, A.; Heinemann, U.; Friedman, A. Blood-brain barrier dysfunction in epileptogenesis of the temporal lobe. *Epilepsy Res. Treat.* **2011**, 143908, doi:10.1155/2011/143908.

7. Abbott, N.J.; Patabendige, A.A.K.; Dolman, D.E.M.; Yusof, S.R.; Begley, D.J. Structure and Function of the Blood-Brain Barrier. *Neurobiol. Dis.* **2010**, *37*, 13–25, doi:10.1016/j.nbd.2009.07.030.

8. Xu, K.; Liu, F.; Xu, W.; Liu, J.; Chen, S.; Wu, G. Transplanting GABAergic Neurons Differentiated from Neural Stem Cells into Hippocampus Inhibits Seizures and Epileptiform Discharges in Pilocarpine-Induced Temporal Lobe Epilepsy Model. *World Neurosurg.* **2019**, *128*, e1–e11, doi:10.1016/j.wneu.2019.01.245.

9. Klein, P.; Dingledine, R.; Aronica, E.; Bernard, C.; Blümcke, I.; Boison, D.; Brodie, M.J.; Brooks-Kayal, A.R.; Engel, J.; Forcelli, P.A.; et al. Commonalities in Epileptogenic Processes from Different Acute Brain Insults: Do They Translate? *Epilepsia* **2018**, *59*, 37–66, doi:10.1111/epi.13965.

10. van Vliet, E.A.; da Costa Araújo, S.; Redeker, S.; van Schaik, R.; Aronica, E.; Gorter, J.A. Blood-Brain Barrier Leakage May Lead to Progression of Temporal Lobe Epilepsy. *Brain J. Neurol.* **2007**, *130*, 521–534, doi:10.1093/brain/awl318.

11. Tomkins, O.; Shelef, I.; Kaizerman, I.; Eliushin, A.; Afawi, Z.; Misk, A.; Gidon, M.; Cohen, A.; Zumsteg, D.; Friedman, A. Blood-Brain Barrier Disruption in Post-Traumatic Epilepsy. *J. Neurol. Neurosurg. Psychiatry* **2008**, *79*, 774–777, doi:10.1136/jnnp.2007.126425.

12. Raabe, A.; Schmitz, A.K.; Pernhorst, K.; Grote, A.; von der Brelie, C.; Urbach, H.; Friedman, A.; Becker, A.J.; Elger, C.E.; Niehusmann, P. Cliniconeuropathologic Correlations Show Astroglial Albumin Storage as a Common Factor in Epileptogenic Vascular Lesions. *Epilepsia* **2012**, *53*, 539–548, doi:10.1111/j.1528-1167.2012.03405.x.

13. van Vliet, E.A.; Otte, W.M.; Gorter, J.A.; Dijkhuizen, R.M.; Wadman, W.J. Longitudinal Assessment of Blood-Brain Barrier Leakage during Epileptogenesis in Rats. A Quantitative MRI Study. *Neurobiol. Dis.* **2014**, *63*, 74–84, doi:10.1016/j.nbd.2013.11.019.

14. Gorter, J.A.; van Vliet, E.A.; Aronica, E. Status Epilepticus, Blood-Brain Barrier Disruption, Inflammation, and Epileptogenesis. *Epilepsy Behav. EB* **2015**, *49*, 13–16, doi:10.1016/j.yebeh.2015.04.047.

15. Maroso, M.; Balosso, S.; Ravizza, T.; Liu, J.; Aronica, E.; Iyer, A.M.; Rossetti, C.; Molteni, M.; Casalgrandi, M.; Manfredi, A.A.; et al. Toll-like Receptor 4 and High-Mobility Group Box-1 Are Involved in Ictogenesis and Can Be Targeted to Reduce Seizures. *Nat. Med.* **2010**, *16*, 413–419, doi:10.1038/nm.2127.

16. Liebner, S.; Dijkhuizen, R.M.; Reiss, Y.; Plate, K.H.; Agalliu, D.; Constantin, G. Functional Morphology of the Blood-Brain Barrier in Health and Disease. *Acta Neuropathol. (Berl.)* **2018**, *135*, 311–336, doi:10.1007/s00401-018-1815-1.

17. Patel, D.C.; Tewari, B.P.; Chaunsali, L.; Sontheimer, H. Neuron-Glia Interactions in the Pathophysiology of Epilepsy. *Nat. Rev. Neurosci.* **2019**, *20*, 282–297, doi:10.1038/s41583-019-0126-4.

18. Shen, W.; Pristov, J.B.; Nobili, P.; Nikolić, L. Can Glial Cells Save Neurons in Epilepsy? *Neural Regen. Res.* **2023**, *18*, 1417–1422, doi:10.4103/1673-5374.360281.

19. Kyriatzis, G.; Bernard, A.; Bôle, A.; Pflieger, G.; Chalas, P.; Masse, M.; Lécorché, P.; Jacquot, G.; Ferhat, L.; Khrestchatisky, M. Neurotensin Receptor 2 Is Induced in Astrocytes and Brain Endothelial Cells in Relation to Neuroinflammation Following Pilocarpine-Induced Seizures in Rats. *Glia* **2021**, *69*, 2618–2643, doi:10.1002/glia.24062.

20. Racine, R.J. Modification of Seizure Activity by Electrical Stimulation. II. Motor Seizure. *Electroencephalogr. Clin. Neurophysiol.* **1972**, *32*, 281–294, doi:10.1016/0013-4694(72)90177-0.

21. Sbai, O.; Ould-Yahoui, A.; Ferhat, L.; Gueye, Y.; Bernard, A.; Charrat, E.; Mehanna, A.; Risso, J.-J.; Chauvin, J.-P.; Fenouillet, E.; et al. Differential Vesicular Distribution and Trafficking of MMP-2, MMP-9, and Their Inhibitors in Astrocytes. *Glia* **2010**, *58*, 344–366, doi:10.1002/glia.20927.

22. Pagano, A.; Breuzard, G.; Parat, F.; Tchoghandjian, A.; Figarella-Branger, D.; De Bessa, T.C.; Garrouste, F.; Douence, A.; Barbier, P.; Kovacic, H. Tau Regulates Glioblastoma Progression, 3D Cell Organization, Growth and Migration via the PI3K-AKT Axis. *Cancers* **2021**, *13*, 5818, doi:10.3390/cancers13225818.

23. Silvani, G.; Romanov, V.; Cox, C.D.; Martinac, B. Biomechanical Characterization of Endothelial Cells Exposed to Shear Stress Using Acoustic Force Spectroscopy. *Front. Bioeng. Biotechnol.* **2021**, *9*, 612151, doi:10.3389/fbioe.2021.612151.

24. Schmidt-Kastner, R.; Ingvar, M. Loss of Immunoreactivity for Glial Fibrillary Acidic Protein (GFAP) in Astrocytes as a Marker for Profound Tissue Damage in Substantia Nigra and Basal Cortical Areas after Status Epilepticus Induced by Pilocarpine in Rat. *Glia* **1994**, *12*, 165–172, doi:10.1002/glia.440120302.

25. Sharma, A.K.; Reams, R.Y.; Jordan, W.H.; Miller, M.A.; Thacker, H.L.; Snyder, P.W. Mesial Temporal Lobe Epilepsy: Pathogenesis, Induced Rodent Models and Lesions. *Toxicol. Pathol.* **2007**, *35*, 984–999, doi:10.1080/01926230701748305.

26. Knake, S.; Hamer, H.M.; Rosenow, F. Status Epilepticus: A Critical Review. *Epilepsy Behav. EB* **2009**, *15*, 10–14, doi:10.1016/j.yebeh.2009.02.027.

27. Papageorgiou, I.E.; Gabriel, S.; Fetani, A.F.; Kann, O.; Heinemann, U. Redistribution of Astrocytic Glutamine Synthetase in the Hippocampus of Chronic Epileptic Rats. *Glia* **2011**, *59*, 1706–1718, doi:10.1002/glia.21217.

28. Uzunalli, G.; Dieterly, A.M.; Kemet, C.M.; Weng, H.-Y.; Soepriatna, A.H.; Goergen, C.J.; Shinde, A.B.; Wendt, M.K.; Lyle, L.T. Dynamic Transition of the Blood-Brain Barrier in the Development of Non-Small Cell Lung Cancer Brain Metastases. *Oncotarget* **2019**, *10*, 6334–6348, doi:10.18632/oncotarget.27274.

29. Mendes, N.F.; Pansani, A.P.; Carmanhães, E.R.F.; Tange, P.; Meireles, J.V.; Ochikubo, M.; Chagas, J.R.; da Silva, A.V.; Monteiro de Castro, G.; Le Sueur-Maluf, L. The Blood-Brain Barrier Breakdown During Acute Phase of the Pilocarpine Model of Epilepsy Is Dynamic and Time-Dependent. *Front. Neurol.* **2019**, *10*, 382, doi:10.3389/fneur.2019.00382.

30. Armulik, A.; Genové, G.; Mäe, M.; Nisancioglu, M.H.; Wallgard, E.; Niaudet, C.; He, L.; Norlin, J.; Lindblom, P.; Strittmatter, K.; et al. Pericytes Regulate the Blood-Brain Barrier. *Nature* **2010**, *468*, 557–561, doi:10.1038/nature09522.

31. Cao, L.; Zhou, Y.; Chen, M.; Li, L.; Zhang, W. Pericytes for Therapeutic Approaches to Ischemic Stroke. *Front. Neurosci.* **2021**, *15*, 629297, doi:10.3389/fnins.2021.629297.

32. Schmidt-Kastner, R.; Ingvar, M. Laminar Damage of Neurons and Astrocytes in Neocortex and Hippocampus of Rat after Long-Lasting Status Epilepticus Induced by Pilocarpine. *Epilepsy Res. Suppl.* **1996**, *12*, 309–316.

33. Garzillo, C.; Mello, L. Characterization of Reactive Astrocytes in the Chronic Phase of the Pilocarpine Model of Epilepsy. *Epilepsia* **2002**, *43 Suppl 5*, 107–109. doi:10.1046/j.1528-1157.43.s.5.40.x

34. Choi, J.; Koh, S. Role of Brain Inflammation in Epileptogenesis. *Yonsei Med. J.* **2008**, *49*, 1–18, doi:10.3349/ymj.2008.49.1.1.

35. Shapiro, L.A.; Wang, L.; Ribak, C.E. Rapid Astrocyte and Microglial Activation Following Pilocarpine-Induced Seizures in Rats. *Epilepsia* **2008**, *49 Suppl 2*, 33–41, doi:10.1111/j.1528-1167.2008.01491.x.

36. Lertkiatmongkol, P.; Liao, D.; Mei, H.; Hu, Y.; Newman, P.J. Endothelial Functions of Platelet/Endothelial Cell Adhesion Molecule-1 (CD31). *Curr. Opin. Hematol.* **2016**, *23*, 253–259, doi:10.1097/MOH.0000000000000239.

37. Yan, B.C.; Xu, P.; Gao, M.; Wang, J.; Jiang, D.; Zhu, X.; Won, M.-H.; Su, P.Q. Changes in the Blood-Brain Barrier Function Are Associated With Hippocampal Neuron Death in a Kainic Acid Mouse Model of Epilepsy. *Front. Neurol.* **2018**, *9*, 775, doi:10.3389/fneur.2018.00775.

38. Rana, A.; Musto, A.E. The Role of Inflammation in the Development of Epilepsy. *J. Neuroinflammation* **2018**, *15*, 144, doi:10.1186/s12974-018-1192-7.

39. Williams, K.C.; Zhao, R.W.; Ueno, K.; Hickey, W.F. PECAM-1 (CD31) Expression in the Central Nervous System and Its Role in Experimental Allergic Encephalomyelitis in the Rat. *J. Neurosci. Res.* **1996**, *45*, 747–757, doi:10.1002/(SICI)1097-4547(19960915)45:6<747::AID-JNR11>3.0.CO;2-T.

40. Privratsky, J.R.; Newman, D.K.; Newman, P.J. PECAM-1: Conflicts of Interest in Inflammation. *Life Sci.* **2010**, *87*, 69–82, doi:10.1016/j.lfs.2010.06.001.

41. Cheung, K.; Ma, L.; Wang, G.; Coe, D.; Ferro, R.; Falasca, M.; Buckley, C.D.; Mauro, C.; Marelli-Berg, F.M. CD31 Signals Confer Immune Privilege to the Vascular Endothelium. *Proc. Natl. Acad. Sci. U. S. A.* **2015**, *112*, E5815-5824, doi:10.1073/pnas.1509627112.

42. Shen, J.; Ishii, Y.; Xu, G.; Dang, T.C.; Hamashima, T.; Matsushima, T.; Yamamoto, S.; Hattori, Y.; Takatsuru, Y.; Nabekura, J.; et al. PDGFR-β as a Positive Regulator of Tissue Repair in a Mouse Model of Focal Cerebral Ischemia. *J. Cereb. Blood Flow Metab. Off. J. Int. Soc. Cereb. Blood Flow Metab.* **2012**, *32*, 353–367, doi:10.1038/jcbfm.2011.136.

43. Iihara, K.; Sasahara, M.; Hashimoto, N.; Hazama, F. Induction of Platelet-Derived Growth Factor Beta-Receptor in Focal Ischemia of Rat Brain. *J. Cereb. Blood Flow Metab. Off. J. Int. Soc. Cereb. Blood Flow Metab.* **1996**, *16*, 941–949, doi:10.1097/00004647-199609000-00018.

44. Krupinski, J.; Issa, R.; Bujny, T.; Slevin, M.; Kumar, P.; Kumar, S.; Kaluza, J. A Putative Role for Platelet-Derived Growth Factor in Angiogenesis and Neuroprotection after Ischemic Stroke in Humans. *Stroke* **1997**, *28*, 564–573, doi:10.1161/01.str.28.3.564.

45. Arimura, K.; Ago, T.; Kamouchi, M.; Nakamura, K.; Ishitsuka, K.; Kuroda, J.; Sugimori, H.; Ooboshi, H.; Sasaki, T.; Kitazono, T. PDGF Receptor β Signaling in Pericytes Following Ischemic Brain Injury. *Curr. Neurovasc. Res.* **2012**, *9*, 1–9, doi:10.2174/156720212799297100.

46. Chintalgattu, V.; Ai, D.; Langley, R.R.; Zhang, J.; Bankson, J.A.; Shih, T.L.; Reddy, A.K.; Coombes, K.R.; Daher, I.N.; Pati, S.; et al. Cardiomyocyte PDGFR-Beta Signaling Is an Essential Component of the Mouse Cardiac Response to Load-Induced Stress. *J. Clin. Invest.* **2010**, *120*, 472–484, doi:10.1172/JCI39434.

47. Klement, W.; Blaquiere, M.; Zub, E.; deBock, F.; Boux, F.; Barbier, E.; Audinat, E.; Lerner-Natoli, M.; Marchi, N. A Pericyte-Glia Scarring Develops at the Leaky Capillaries in the Hippocampus during Seizure Activity. *Epilepsia* **2019**, *60*, 1399–1411, doi:10.1111/epi.16019.

15

48. Sakai, K.; Takata, F.; Yamanaka, G.; Yasunaga, M.; Hashiguchi, K.; Tominaga, K.; Itoh, K.; Kataoka, Y.; Yamauchi, A.; Dohgu, S. Reactive Pericytes in Early Phase Are Involved in Glial Activation and Late-Onset Hypersusceptibility to Pilocarpine-Induced Seizures in Traumatic Brain Injury Model Mice. *J. Pharmacol. Sci.* **2021**, *145*, 155–165, doi:10.1016/j.jphs.2020.11.008.

49. Arango-Lievano, M.; Boussadia, B.; De Terdonck, L.D.T.; Gault, C.; Fontanaud, P.; Lafont, C.; Mollard, P.; Marchi, N.; Jeanneteau, F. Topographic Reorganization of Cerebrovascular Mural Cells under Seizure Conditions. *Cell Rep.* **2018**, *23*, 1045–1059, doi:10.1016/j.celrep.2018.03.110.

50. Garbelli, R.; de Bock, F.; Medici, V.; Rousset, M.C.; Villani, F.; Boussadia, B.; Arango-Lievano, M.; Jeanneteau, F.; Daneman, R.; Bartolomei, F.; et al. PDGFRβ(+) Cells in Human and Experimental Neuro-Vascular Dysplasia and Seizures. *Neuroscience* **2015**, *306*, 18–27, doi:10.1016/j.neuroscience.2015.07.090.

51. Milesi, S.; Boussadia, B.; Plaud, C.; Catteau, M.; Rousset, M.-C.; De Bock, F.; Scheffer, M.; Lerner-Natoli, M.; Rigau, V.; Marchi, N. Redistribution of PDGFRβ Cells and NG2DsRed Pericytes at the Cerebrovasculature after Status Epilepticus. *Neurobiol. Dis.* **2014**, *0*, 151–158, doi:10.1016/j.nbd.2014.07.010.

52. Yamanaka, G.; Takata, F.; Kataoka, Y.; Kanou, K.; Morichi, S.; Dohgu, S.; Kawashima, H. The Neuroinflammatory Role of Pericytes in Epilepsy. *Biomedicines* **2021**, *9*, 759, doi:10.3390/biomedicines9070759.

53. Michalski, D.; Spielvogel, E.; Puchta, J.; Reimann, W.; Barthel, H.; Nitzsche, B.; Mages, B.; Jäger, C.; Martens, H.; Horn, A.K.E.; et al. Increased Immunosignals of Collagen IV and Fibronectin Indicate Ischemic Consequences for the Neurovascular Matrix Adhesion Zone in Various Animal Models and Human Stroke Tissue. *Front. Physiol.* **2020**, *11*, 575598, doi:10.3389/fphys.2020.575598.

54. Christensen, N.M.; Trevisan, C.; Leifsson, P.S.; Johansen, M.V. The Association between Seizures and Deposition of Collagen in the Brain in Porcine Taenia Solium Neurocysticercosis. *Vet. Parasitol.* **2016**, *228*, 180–182, doi:10.1016/j.vetpar.2016.09.008.

55. Liesi, P.; Kauppila, T. Induction of Type IV Collagen and Other Basement-Membrane-Associated Proteins after Spinal Cord Injury of the Adult Rat May Participate in Formation of the Glial Scar. *Exp. Neurol.* **2002**, *173*, 31–45, doi:10.1006/exnr.2001.7800.

56. Özkan, E.; Çetin-Taş, Y.; Şekerdağ, E.; Kızılırmak, A.B.; Taş, A.; Yıldız, E.; Yapıcı-Eser, H.; Karahüseyinoğlu, S.; Zeybel, M.; Gürsoy-Özdemir, Y. Blood-Brain Barrier Leakage and Perivascular Collagen Accumulation Precede Microvessel Rarefaction and Memory Impairment in a Chronic Hypertension Animal Model. *Metab. Brain Dis.* **2021**, *36*, 2553–2566, doi:10.1007/s11011-021-00767-8.

57. Veznedaroglu, E.; Van Bockstaele, E.J.; O'Connor, M.J. Extravascular Collagen in the Human Epileptic Brain: A Potential Substrate for Aberrant Cell Migration in Cases of Temporal Lobe Epilepsy. *J. Neurosurg.* **2002**, *97*, 1125–1130, doi:10.3171/jns.2002.97.5.1125.

58. Lowenstein, D.H.; Arsenault, L. Dentate Granule Cell Layer Collagen Explant Cultures: Spontaneous Axonal Growth and Induction by Brain-Derived Neurotrophic Factor or Basic Fibroblast Growth Factor. *Neuroscience* **1996**, *74*, 1197–1208, doi:10.1016/0306-4522(96)00226-6.

59. Hoeppner, T.J.; Morrell, F. Control of Scar Formation in Experimentally Induced Epilepsy. *Exp. Neurol.* **1986**, *94*, 519–536, doi:10.1016/0014-4886(86)90235-9.